Journal of Power Sources 196 (2011) 7175–7181

Contents lists available at ScienceDirect

Journal of Power Sources

journal homepage: www.elsevier.com/locate/jpowsour

Investigation of solid oxide fuel cell sealing behavior under stack relevant conditions at Forschungszentrum Jülich

Ludger Blum*, Sonja M. Groß, Jürgen Malzbender, Ulrich Pabst, Murat Peksen, Roland Peters, Izaak C. Vinke

Forschungszentrum Jülich GmbH, Wilhelm-Johnen-Straße, D-52428 Jülich, Germany

ARTICLE INFO

Article history:
Received 27 June 2010
Received in revised form
15 September 2010
Accepted 16 September 2010
Available online 24 September 2010

Keywords:
Solid oxide fuel cell (SOFC)
Stack
Sealing
Finite element modelling

ABSTRACT

Hermetic sealing is a key requirement for the operation of solid oxide fuel cell (SOFC) stacks in a system environment. The sealant material has to withstand stresses due to mechanical loading, mismatch in thermal expansion coefficient and thermal gradients that arise during operation. Based on leakage tests performed at Forschungszentrum Jülich it was obvious that stacks, having been operated successfully in a furnace, are not necessarily usable in a system, e.g. because of deviating pressure differences and temperature gradients. Thorough investigations including stack and stack dummy tests, and finite element modeling (FEM) were performed to get a comprehensive understanding of the various parameters, influencing the leak tightness of the sealing material. It was found that even small temperature differences especially in the area of gas and air manifolds can create excessively high tensile stresses. Based on initial FEM analyses, a better understanding of the problem has been obtained and a tool was developed that can assist in the design of more robust stacks. These investigations and modeling activities will be continued with a main focus on thermal cycling, which is the next step in the list of requirements.

1. Introduction

Gas tightness of SOFC stacks is a severe but indispensable pre-requisite for reliable and long term stable operation. In most cases sealing is realized using specifically developed glass ceramics, metallic sealants or flat sealings based on mica. These sealings have to withstand high temperatures combined with oxidizing and reducing atmospheres as well as the mechanical stress caused by temperature gradients during operation and thermal cycling. Moreover, the sealing has to be electrically insulating (otherwise an additional insulation layer has to be applied). Remarkable development has been done in this field, as reported for example, in [1–4].

In the stack design used in Jülich, three layers of glass ceramic are present, as illustrated in Fig. 1:

- sealing the metal frame (including manifold) to the anode side of the interconnect plate (electrical insulation not required);
- sealing the metal frame (including manifold) to the cathode side of the interconnect plate (electrical insulation required);
- sealing the cell outer rim to the interconnect plate (electrical insulation required).

Because of the integrated manifold combined with counter-/co-flow design the manifold sealing is the largest part of the total sealing area.

As reported in [5], Jülich was able to operate stacks up to 60 layers based on a design (denoted as F20), incorporating these features, using cells of 20 cm × 20 cm substrate size. These anode substrate cells use Ni-YSZ anode, 8YSZ electrolyte and LSM or LSCF cathode. All these stacks have been operated in a furnace, which implies low pressure differences between the gases and the environment, and no safety problems with small leakages, because they are immediately burned inside the furnace.

Based on these results, 5 kW stacks were planned to be integrated in the 20 kW system, as described in [6]. These were manufactured and pre-tested electrically in a furnace.

After having ensured the required electrical performance, leakage tests performed at room temperature revealed a leakage rate from the fuel chamber to the environment 10 times higher than the allowed one. The allowed limit of leakage was set to be 1% of the fuel flow (reformed methane with S/C of 2.2) at nominal operating con-

Abbreviations: CFD, computational fluid dynamics; FEM, finite element modelling; S/C, steam to carbon ratio (mole per mole); SOFC, solid oxide fuel cell; u_F, utilization of fuel.

* Corresponding author. Tel.: +49 2461 61 6709; fax: +49 2461 61 6695.
E-mail addresses: l.blum@fz-juelich.de (L. Blum), s.m.gross@fz-juelich.de (S.M. Groß), j.malzbender@fz-juelich.de (J. Malzbender), u.pabst@fz-juelich.de (U. Pabst), m.peksen@fz-juelich.de (M. Peksen), ro.peters@fz-juelich.de (R. Peters), i.c.vinke@fz-juelich.de (I.C. Vinke).

0378-7753/$ – see front matter © 2010 Elsevier B.V. All rights reserved.
doi:10.1016/j.jpowsour.2010.09.041

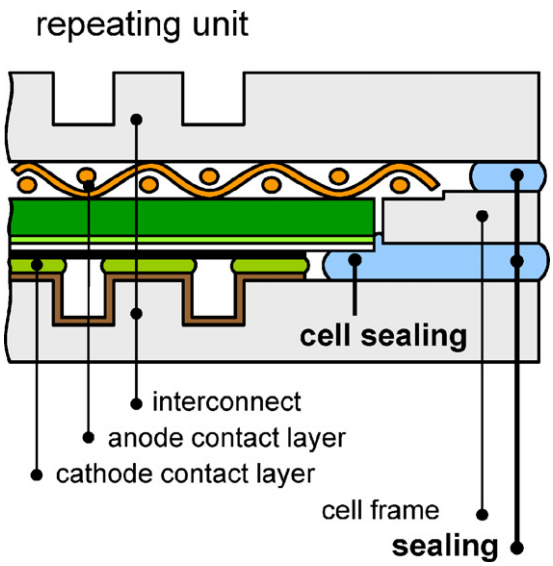

Fig. 1. Design concept of Jülich F-Design Stacks.

ditions (0.5 A cm^{-2} at a fuel utilization of 70%). The leakage rate was calculated for a pressure difference between fuel and environment of 150 mbar, which results from the system operation.

Several possible reasons for the leakage were discussed:

- Properties of furnace or adapter plate
- Clamping of the stack
- Handling
- Size of cells and plates
- Evenness of interconnect plates
- Dimensions and shape of manifold (round/angular with different ratios)

2. Scientific approach

To simplify the test and to avoid the influence of the cells (mechanical properties, electrochemical behavior), it was decided to investigate the sealing using dummy stacks built of original stack components, and replacing the cells by metal sheets of the same dimensions. The dummy normally contained 11 sealing layers (being equivalent to five dummy cells). The units were sealed in a furnace, according to the standard procedure. After cooling down to ambient temperature a leakage test was performed in the furnace, and after removing the dummy from the furnace, in a special test bench. For post mortem analysis the dummy was impregnated with a penetrating dye to identify the location of leakage. For a better understanding of the thermo-mechanical behavior, finite element analysis was performed using measured and calculated temperature profiles as input.

3. Experiments and modelling

Thorough investigations of the stacks revealed that the main leakage occurred in the manifold area via cracks in the glass ceramic sealant. Initial tests revealed that the furnace could not be the reason for the stack leakage. Also clamping and handling did not appear to affect the leakage rate. In fact dummy stacks which had been gas tight could be removed from the furnace with and without clamping, and could be transported and integrated into the leakage test equipment again without change of gas tightness. Tests with only one sealing layer but with the same outer dimensions as the F20 stack (Dummy 5–7) showed the same very low leakage rates of 10^{-9} mbar l s^{-1} as small samples of 5 cm × 5 cm, which have been used to characterize the different glass ceramic materials. This implied that not the larger size itself caused the problems. The same holds for the shape of the manifold. Samples of 10 cm × 10 cm with different manifold designs also showed leakage rates of 10^{-9} mbar l s^{-1}. Also a dummy stack with uneven inter-

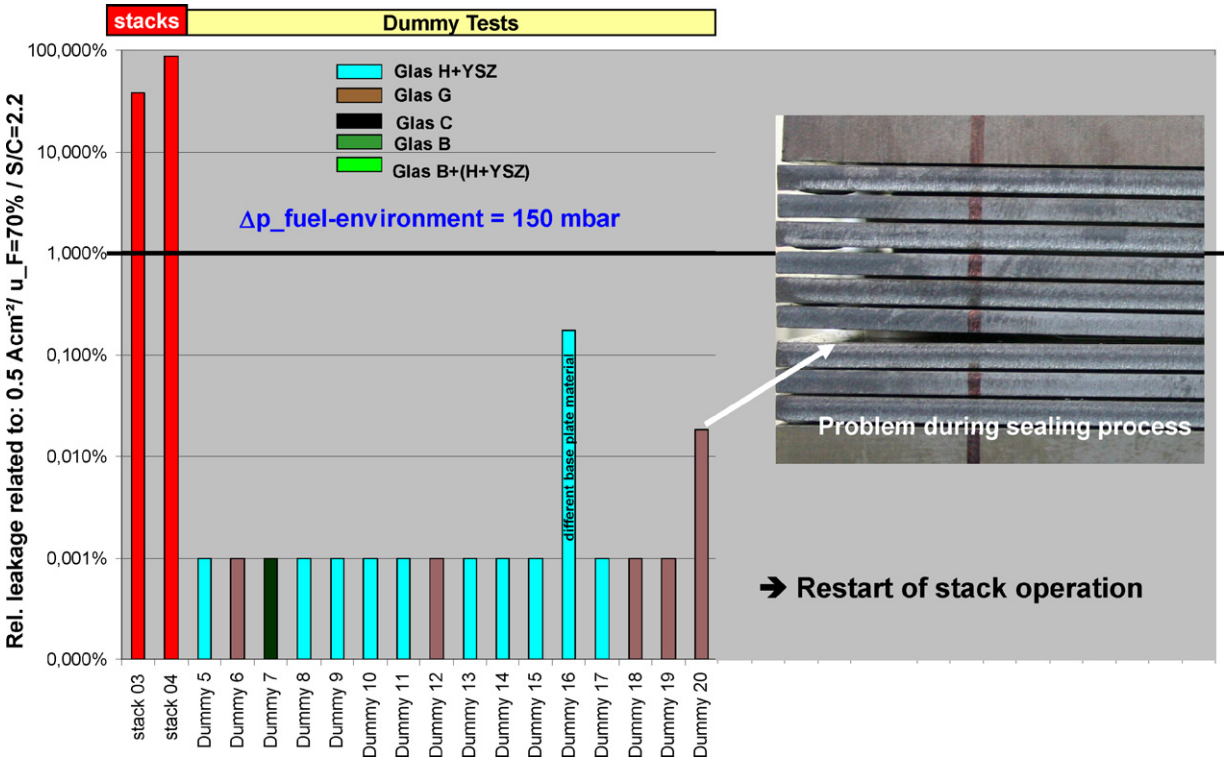

Fig. 2. Leakage rates of the first stack and dummy tests.

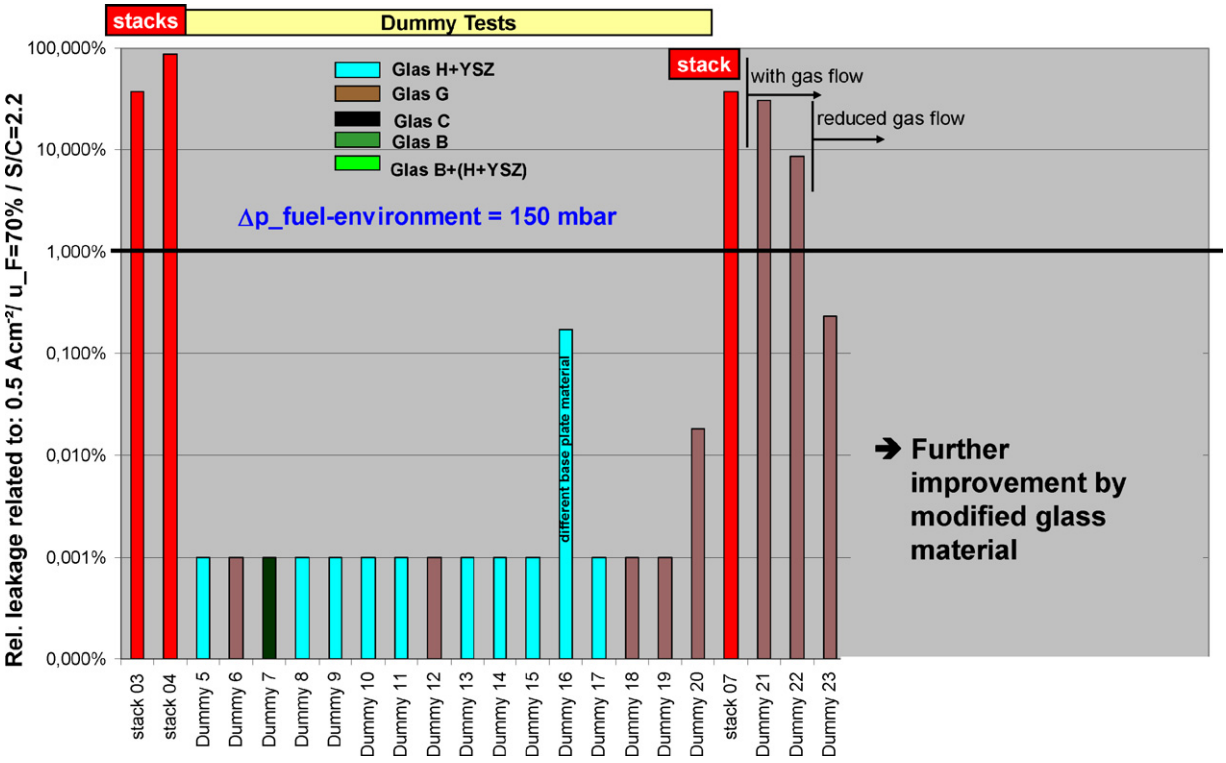

Fig. 3. Leakage rates of stack and dummy tests with and without gas flow.

connect plates (outside specification) did not show an effect on the leakage rate (Dummy 15). The results of the dummy tests up to No. 20 are shown in Fig. 2. Only two tests showed increased leakage rates because of special problems (different base plate material with bad adhesion to the glass ceramic material and one mechanical problem during sealing process, which was sticking on a locating pin). All the other tests showed very good gas tightness, also for different types of glasses.

As a result, none of the possible reasons stated above could be identified as an explanation for the leakage.

Having ascertained no further reason for gas leakage, it was decided to restart the stack manufacturing after Dummy 20, using

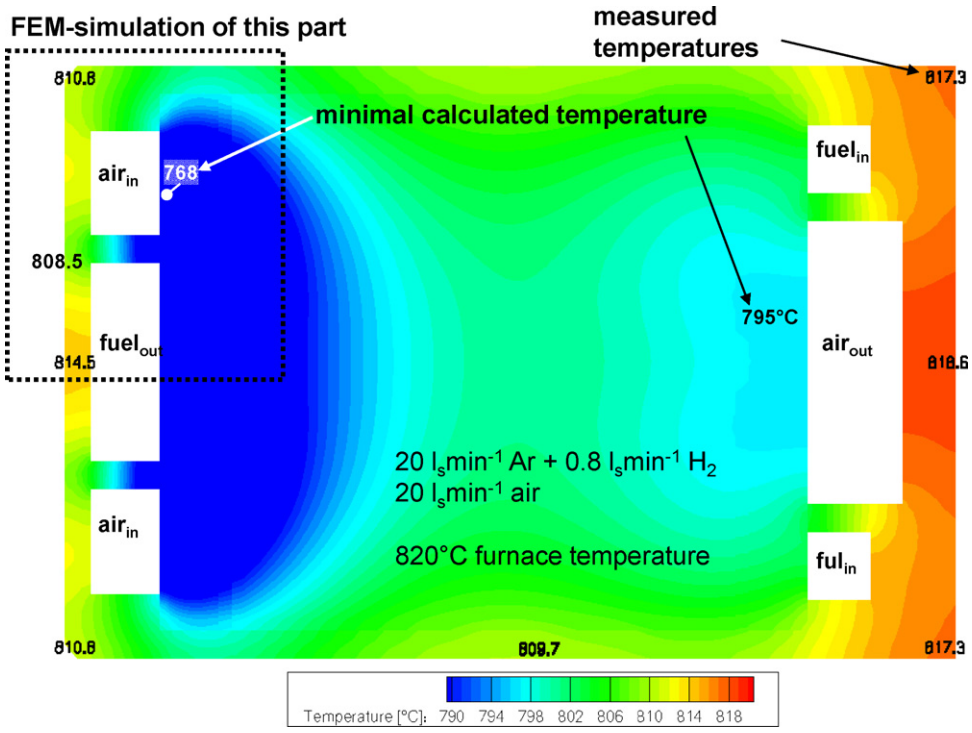

Fig. 4. Temperature distribution in a dummy stack after sealing process with T_{air_in} = 165 °C; T_{fuel_in} = 225 °C.

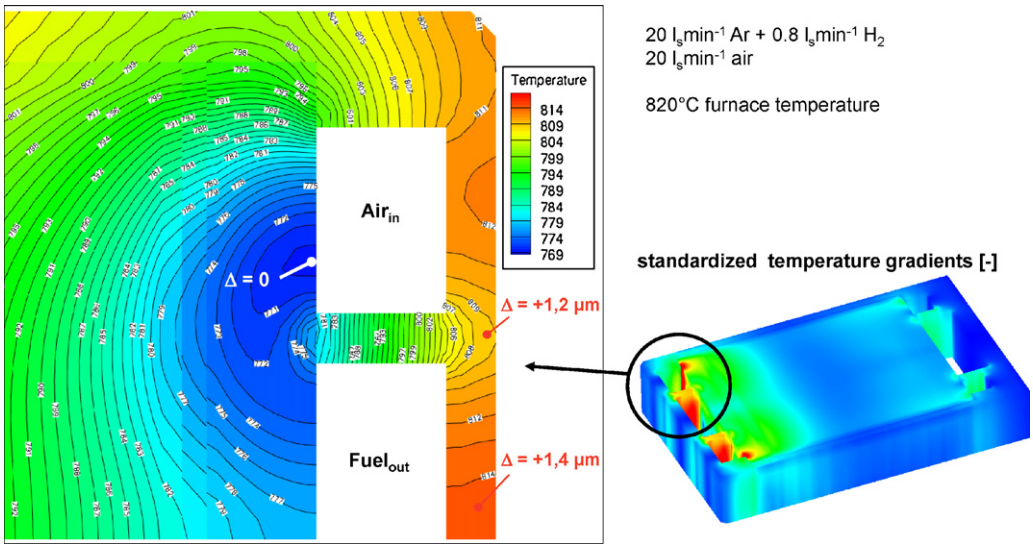

Fig. 5. Temperature distribution in the air inlet zone of a dummy stack after sealing process and the resulting standardized temperature gradients.

the glass ceramic material, which possessed the best mechanical strength at room temperature (glass G).

However, the stack (F″2010-07) showed a high leakage rate comparable to the initial stacks. The only remaining difference to the dummy test was the gas flow, which was applied during stack commissioning to avoid the oxidation of the nickel mesh and to reduce the anode after the sealing process. This was not done with the dummy stacks, for easier separation of effects.

The next two dummy stacks, operated with gas flow comparable to the stack, showed the same leakage rates as the stack. In a follow up test, the gas flow was reduced to the possible minimum and the leakage rate could be reduced by two orders of magnitude. The leakage was below the required limit but still much higher than it was observed without gas flow (see Fig. 3).

Now a two way strategy was followed to improve the situation further. On the one hand finite element modeling (FEM) should reveal the reasons for the leakage; on the other hand, improved glass ceramic material was tested.

Based on temperature measurements undertaken in a dummy stack during operation with gas flow, the temperature distribution was calculated using a 3D-CFD model. The dummy was operated at a furnace temperature of 820 °C loaded on the cathode side with an air flow of 20 standard liters per minute, pre-heated to 165 °C, and with a flow of argon on the anode side of 20 standard liters per minute mixed with 0.8 standard liters per minute of hydrogen, pre-heated to 225 °C. These low gas temperatures create a maximal temperature difference in the manifold area of an interconnect plate of about 46 K on the air inlet side and about 24 K on the fuel inlet side (see Fig. 4). These differences are similar to the values created during stack operation. In Fig. 5, a more detailed temperature distribution and the resulting standardized temperature gradients are shown. The red numbers in the figure indicate the changes in thickness of the 2.5 mm thick metal plate, depending on the local temperature in relation to the lowest temperature in that area. Referring to that position, this thickness difference is up to 1.4 µm.

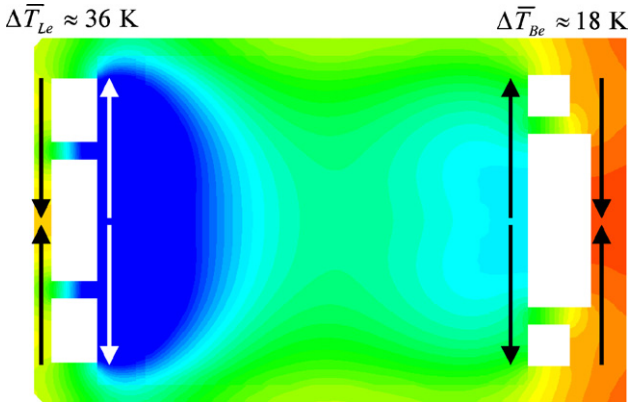

Fig. 7. Mean temperature differences resulting in tensile/compression stress within the layer.

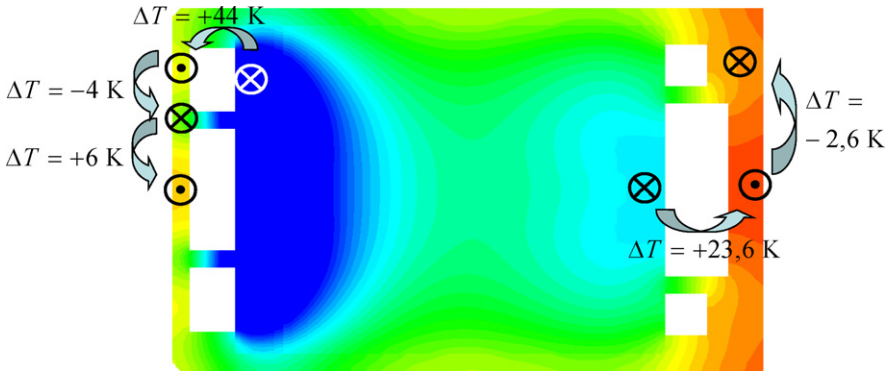

Fig. 6. Local temperature differences resulting in tensile/compression stress perpendicular to the layer.

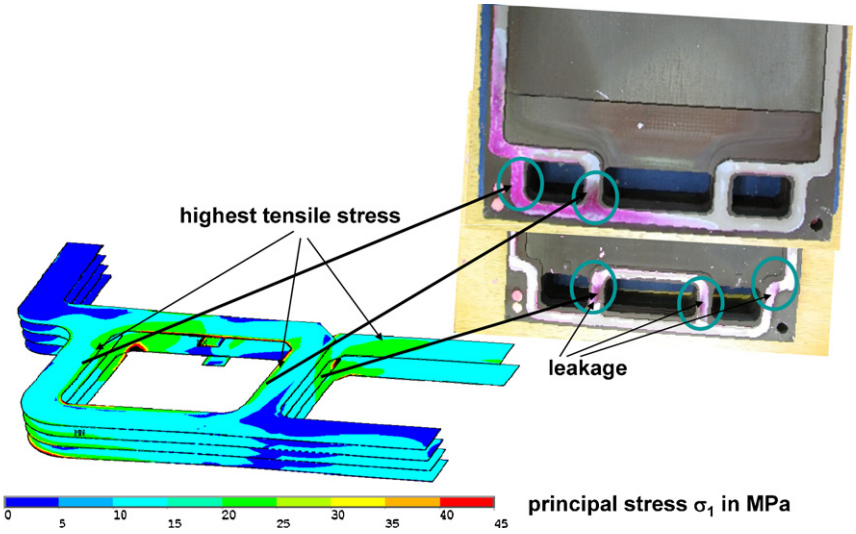

Fig. 8. Results of FEM: principal stress distribution and interconnect plates with found leakage.

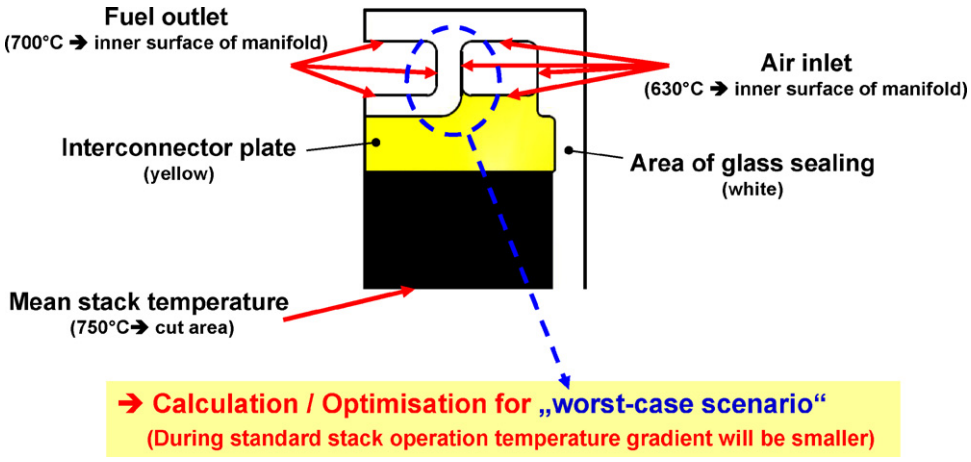

Fig. 9. FEM analysis concept to optimize stack design with respect to a part of the interconnect plate.

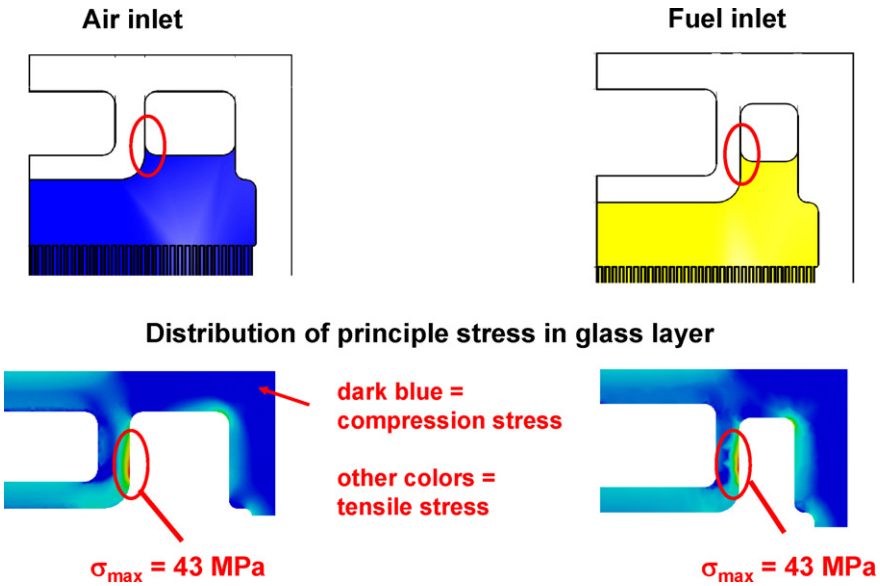

Fig. 10. FEM analysis of basic design: distribution of principle stress in air and fuel inlet manifold.

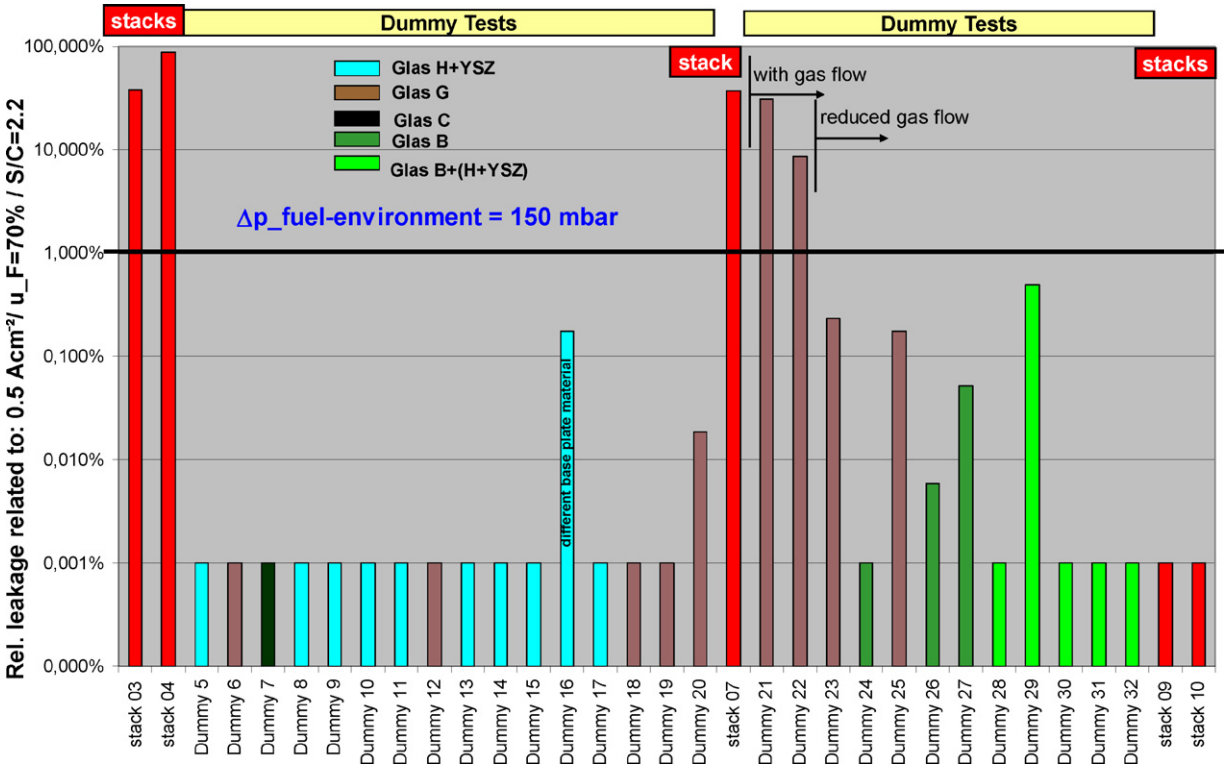

Fig. 11. Leakage rates of stack and dummy tests.

This suggests two different reasons for the thermo-mechanical stress:

- Based on the thickness difference stress is created perpendicular to the layer (see Fig. 6).
- Based on the different mean temperatures inside and outside the manifold holes and the associated different thermal expansion in-plane stress within the layer is created (see Fig. 7).

Initial FEM results using some simplifications (like constant temperature in the thickness direction of the dummy; calculation of only one fourth of the plate because of symmetry reasons) showed, that in some parts of the plate tensile stress is created, and in fact the location of the highest principle stress corresponds quite well with the location of leakage. These positions have been identified experimentally by implementing the method of impregnating the dummy stacks with a penetrating dye to make the cracks visible, after dismantling the dummy as illustrated in Fig. 8. Because of the larger temperature differences in the part of air inlet compared to fuel inlet, the stress is much higher on the air inlet side. This corresponds very well with the results of dummy tests, where most of the leaks could be found in this position.

Table 1
Effect of possible mechanisms on the sealing behavior.

Mechanism	Effect
Influence of furnace (mechanics, temp. distribution)	No
Influence of handling	No
Residual stresses in plates	No
Properties of glass material	Yes; glass B with best results
Thickness of glass sealing	Second order
Influence of plate size	Yes, but only in case of gas flow
Influence of gas flow	Essential (stress resulting from temperature distribution)

Based on these observations, further FEM was carried out to identify critical design features, which cause high tensile stresses. For this purpose again one fourth of a stack plate was modeled impressing a temperature profile representing the worst case scenario during stack operation (see Fig. 9). The resulting principle stress distribution, as shown in Fig. 10, corresponds quite well with that calculated for the dummy stack (Fig. 8) but on a higher stress level because of the larger temperature differences.

In a next step, the entire geometry was parameterized and using a complimentary statistical method, all geometrical features were varied interdependently in order to identify the geometric parameters with the strongest influence on the tensile stress level. Based on these findings an improved design was developed with a decrease in tensile stress by about 60%.

Details of this study based on [7,8] will be reported elsewhere.

Simultaneously to these FEM activities improved glass ceramic sealant materials were tested. Since the operation with reduced gas flow (leading to reduced temperature differences and hence reduced tensile stress as verified by the FEM analysis) has already shown improved gas tightness, this method was used further with a different glass ceramic (glass B), having a better adapted thermal expansion coefficient and higher sealing temperature. Dummy 24 was the first dummy test with gas flow showing comparable tightness to dummy stacks without gas flow. The worst result obtained with glass G was repeated with Dummy 25. With Dummy 26 and 27 (and also 29) modified application procedure and deposited glass amount were tested, again resulting in increased leakage. To further improve the sealing behavior, a combination of two glass ceramics was implemented, using glass B for the manifold sealing and glass H (+YSZ) for the cell sealing (see Fig. 1). Based on this variation, very good sealing results could be obtained. So, two 10 layer stacks were manufactured in the same way also showing very good gas tightness, as depicted in Fig. 11. This now represents the basis for the stacks to be manufactured for the integration in the 20 kW system.

4. Results and conclusions

With the aid of these investigations, mainly based on the use of dummy stacks and on the corresponding finite element modeling, the correlations, presented in Table 1, could be identified. Since the mechanical strength of the glass ceramic sealant materials used so far is relatively low, even small temperature differences especially in the area of gas and air manifolds can create excessively high tensile stresses. Based on initial FEM analyses, a better understanding of the problem has been obtained and a tool was developed that can assist in the design of more robust stacks. Further work is in progress to develop glass materials with improved mechanical strength.

These investigations and modeling activities will be continued with a main focus on thermal cycling, which is the next step in the list of requirements.

Acknowledgements

The authors gratefully thank all the colleagues in the different institutes of Forschungszentrum Jülich, assisting these investigations with their sound knowledge and commitment.

References

[1] E. Wanko, S. Groß, T. Koppitz, J. Remmel, U. Reisgen, W. Wilsmann, R. Conradt, DVS Berichte 243 (2007) 130–134.
[2] S.M. Gross, U. Reisgen, Schweißen und Schneiden 2 (2007) 70–77.
[3] D. Gödeke, J. Besinger, Y. Pflügler, B. Ruedinger, ECS Transactions 25 (2) (2009) 1483–1490.
[4] C.-K. Lina, L.-H. Huanga, L.-K. Chiangb, Y.-P. Chyoub, ECS Transactions 25 (2) (2009) 349–358.
[5] L. Blum, H.-P. Buchkremer, S.M. Gross, L.G.J. de Haart, W.J. Quadakkers, U. Reisgen, R. Steinberger-Wilckens, R.W. Steinbrech, F. Tietz, ECS Transactions 7 (2005) 39.
[6] L. Blum, Ro. Peters, P. David, S.F. Au, R. Deja, W. Tiedemann, Proceedings of the 6th European SOFC Forum, Luzern/CH, 2004, pp. 173–182.
[7] M. Peksen, Ro. Peters, L. Blum, D. Stolten, ECS Transactions 25 (2) (2009) 1195–1200.
[8] M. Peksen, Brennstoffzellenmodul, PT-DE 102010003643.9.